Preliminary Design Description for a First-Generation Liquid-Salt VHTR with Metallic Vessel Internals (AHTR-MI)

Per F. Peterson, Haihua Zhao
U.C. Berkeley
Report UCBTH-05-005

This report will be updated further in 2006
Please contact UCB for subsequent revisions
Rev. E

December 29, 2005

CONTENTS

1.0 INTRODUCTION

The Liquid-Salt Very High Temperature Reactor (LS-VHTR) is a liquid-salt cooled, solid fuel reactor with a nominal thermal power of 2400 MW(t) and power conversion efficiency ranging from 45% to 58% depending on the primary coolant temperature selected, commonly referred to as the Advanced High Temperature Reactor (AHTR) [1]. This report describes design features of a first-generation LS-VHTR that uses metallic reactor vessel internals (AHTR-MI). The primary design goal for the AHTR-MI is to achieve low electricity generation cost compared to Gen III+ LWRs and low technical risk to enable early commercial deployment. Normally materials testing and qualification requirements set the critical path for the development of innovative reactors. The AHTR-MI bypasses this issue by selecting sufficiently low operating temperatures for the prototype plant to allow the use materials that are already ASME code qualified. This strategy allows early commercialization for electricity production, and provides for subsequent increases in the core outlet temperature, enabling upgrade paths for further cost reduction, for production of hydrogen and desalinated water, and for actinide management.

Clean liquid fluoride salts have a number of highly positive attributes for high-temperature heat transfer: , high volumetric heat capacity compared to gases and sodium, high Prandtl numbers that mitigate thermal shock phenomena, transparency similar to water and gases, very low vapor pressures, and very low corrosion rates with graphite and high-nickel alloys under conditions employing effective chemistry control. Traditionally, the major disadvantages of liquid salts have been their high freezing temperatures that resulted in highly complex steam-generator designs, typically from 390°C to 500°C, and their potential corrosiveness when used as solvents for molten salt fuels. The AHTR bypasses the freezing issue by using a high-temperature, closed gas Brayton cycle for power conversion, and bypasses liquid fuel corrosion by using solid fuel.

The AHTR-MI differs significantly from earlier AHTR designs and the current LS-VHTR, because it uses a *closed* primary loop immersed in a reactor tank containing a separate buffer salt. The AHTR-MI primary loop is constructed from metallic materials, and minimizes the total primary salt volume as shown schematically in Fig. 1-1. As with gas-cooled reactors, the coated-particle fuel in the AHTR-MI has large thermal inertia, but the AHTR-MI derives yet greater thermal inertia due to the high volumetric heat capacity of the primary salt, and due to effective natural-circulation heat transfer from the primary salt to a larger mass of buffer salt in a large reactor tank.

Under forced cooling, the AHTR-MI primary loop operates in forced circulation, transferring heat to four intermediate liquid salt loops using modular, compact intermediate heat exchangers located in the reactor tank. Also integrated into the IHX modules is a section of the heat transfer surface that allows heat rejection to the buffer salt. Downstream of the IHX modules are the four primary pumps, which recirculate the primary salt to the reactor core inlet.

Under loss of forced primary circulation, buoyancy forces drive a natural circulation flow of 1% to 2% of normal primary-loop flow. Reduced heat transfer in both the reactor core and IHX modules causes the core temperatures to rise, stopping fission even if

reactor scram does not occur. If intermediate loop heat removal is continued, natural circulation continues to occur through the IHX modules. If intermediate loop heat removal is stopped, heat rejection occurs to the buffer salt, through Pool Reactor Auxiliary Cooling System (PRACS) heat exchangers. As shown in Fig. 1-1, these PRACS loops include a fluidic diode, which reduces leakage flows under primary loop forced circulation. Fluidic diodes are simple, passive devices that provide large flow resistance in one direction, and have been used in nuclear applications for the British Advanced Gas Reactor [1.3].

The PRACS heat exchanger area is sized to match decay heat generation approximately 1 to 2 hours after loss of forced cooling and circulation occurs. Heat removal from the buffer salt to the environment occurs dominantly through Direct Reactor Auxiliary Cooling System (DRACS) heat exchangers, with some heat removal also occurring through the reactor tank cavity cooling system. The DRACS heat removal systems are sized to match decay heat generation approximately 24 to 48 hours after loss of forced cooling and forced circulation occurs.

Design experience with DRACS heat removal systems exists for both the Experimental Breeder Reactor (EBR-II) and the European Fast Reactor (EPR). Conversely, the S-PRISM sodium fast reactor uses a Reactor Vessel Auxiliary Cooling System (RVACS) for decay heat removal. The AHTR-MI has selected the modular PRACS/DRACS decay heat removal system, rather than an integrated RVACS, because it allows the decay heat removal capacity to be scaled independent of the reactor vessel size. This approach greatly reduces the distortion in the design of reduced area Integral Effects Test (IET) experiments for the AHTR-MI, that are required for reactor licensing.

Analysis has not yet been performed to determine the peak core outlet temperature at the time that decay heat generation matches decay heat removal to the intermediate loop, however, a simple lumped mass model for the system indicates that total temperature rise in the system can be restricted to approximately 100°C.

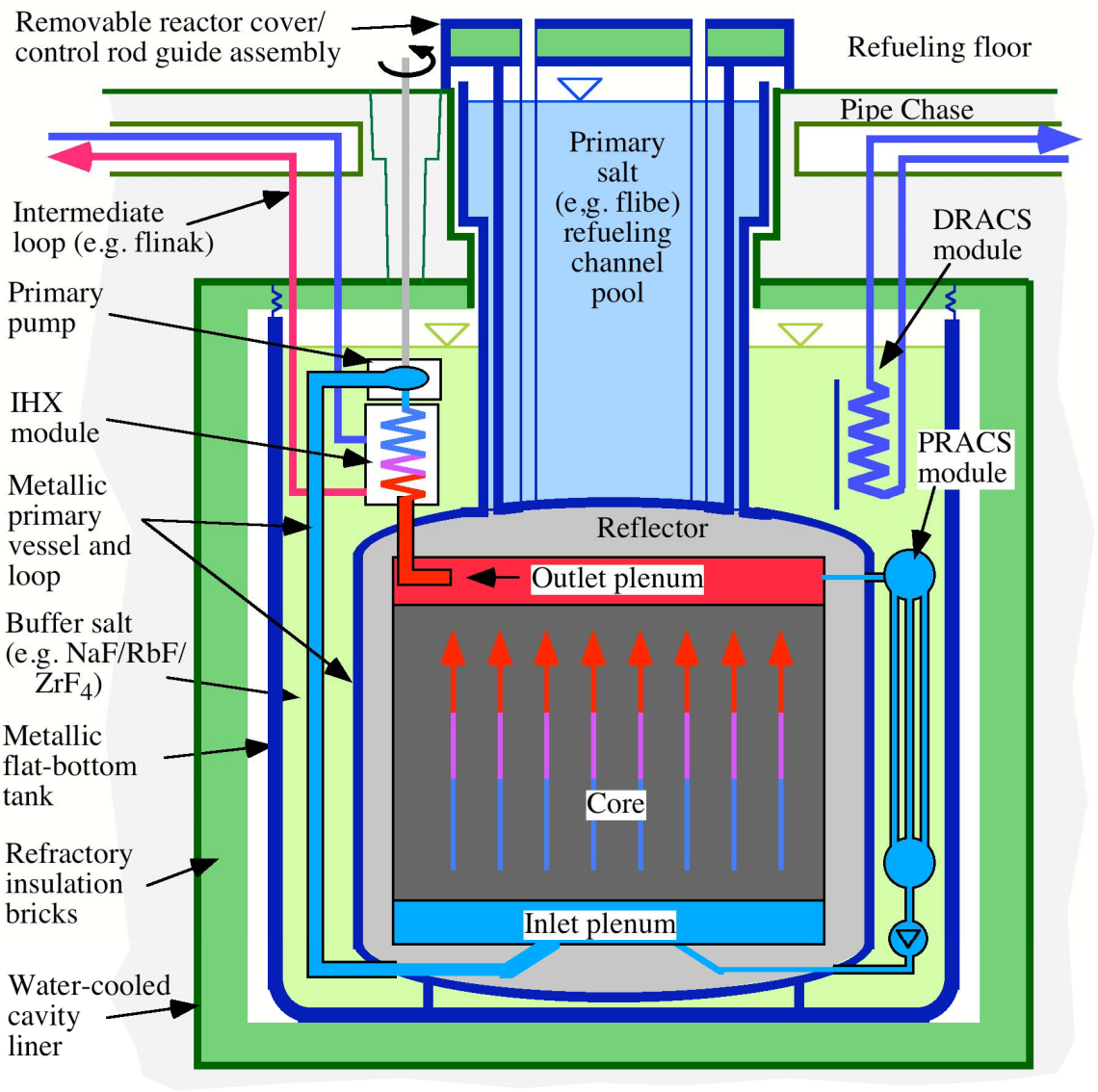

Fig. 1-1 Schematic view of the flow distribution in an AHTR-MI with metallic reactor vessel internals, for power operation.

The remaining sections of this chapter summarize the new features introduced in the AHTR-MI design, make comparisons of the major AHTR-MI design parameters with those of the European Pressurized Reactor to show the basis for predictions of large capital cost reduction, and review the subsequent upgrade pathways for further economics improvements, production of hydrogen and desalinated water, and actinide management. Subsequent chapters describe the major subsystems and present performance and accident response analysis.

1.1 Summary of New AHTR-MI Design Features

The AHTR-MI introduces several new design features that differentiate it from earlier AHTR designs [1.1]. Specifically, the AHTR-MI:

1) Separates the primary loop salt from a larger mass of buffer salt in the reactor tank, allowing different, optimal salt compositions to be used for the primary, buffer, and intermediate salt applications. Under this revised design, forced and natural circulation operation in the AHTR-MI more closely matches that in pressurized water reactors (PWRs) than pool-type sodium fast reactors (SFR) such as S-Prism.

2) Uses metallic construction for the primary loop boundary, pumps, IHX and reactor tank. All metallic components, except the IHX, operate at or below the reactor core inlet temperature under normal operation. Under loss of forced cooling, only the IHX, primary pumps, and PRACS heat exchangers operate at the core outlet temperature, while the other primary loop structures remain close to the buffer-salt temperature.

3) Uses a seismically base isolated, water-cooled, refractory lined reinforced concrete reactor cavity and a flat-bottomed, un-insulated reactor tank to contain the buffer salt. The water-cooled reactor silo liner eliminates the requirement for a guard vessel while minimizing the free volume between the tank and cavity walls.

4) Operates at conservatively low temperatures to allow the use of existing ASME-code qualified materials for all components. An upgrade path then exists to increase the core outlet temperature using advanced IHX, primary pump and PRACS materials.

5) Uses compact, metallic Heatric-type intermediate heat exchangers located in the reactor tank to reduce the primary salt volume, hot and cold leg lengths, and radiation shielding requirements.

6) Uses a combination of PRACS and DRACS heat exchangers to provide modularity decay heat removal following loss of forced cooling, allowing the AHTR's thermal power to be scaled independently from the reactor tank size and greatly simplifying the design of integral effects test facilities.

The AHTR-MI design reduces technical risk by using very low operating temperatures compared to those proposed for high-temperature gas cooled reactors, while achieving comparable power conversion efficiency by using multiple-reheat closed Brayton cycle power conversion. Table 1-1 shows the range of temperatures considered for the first-generation AHTR-MI design.

Table 1-1 Component temperature design range for the AHTR-MI.

Component	Normal Operation	Maximum Transient
Water cooled cavity liner	30-40 °C	100-110 °C
Reactor tank/buffer salt	520-620 °C	750-850 °C
Core inlet	550-650°C	750-850°C
Core outlet (near-term goal)	700-750°C	800-900°C
Core outlet (long-term goal)	750-1000°C	800-1200°C

1.2 Comparison of the AHTR-MI to the Gen III+ EPR

The near-term goal of the AHTR-MI is to provide a large reduction in production cost for electricity compared to the Generation III+ light water reactors that will be the major focus for near-term commercial deployment worldwide. Therefore, while the original capital cost estimates for the AHTR were generated by comparisons to the GT-MHR and S-PRISM reactors [1.2], the capital cost reduction achieved by the AHTR-MI is estimated by comparison with Gen III+ light water reactors. Because the AHTR-MI uses a closed primary loop, several of its key parameters can be compared directly to current pressurized water reactor designs. Table 1-2 shows a comparison of key system parameters for the AHTR-MI and the European Pressurized Reactor (EPR).

1) The AHTR-MI primary loop, IHX, pumps and reactor vessel operate at a pressure 6 times lower than the EPR, allowing the use of thin-walled piping, vessel, and pump casing components with improved thermal shock resistance. The high Prandtl number of the AHTR-MI coolant further reduces thermal shock potential. However, on the negative side the AHTR-MI uses a compact intermediate heat exchanger (IHX) that has higher thermal shock potential than the EPR steam generators.

2) The 4 AHTR-MI primary pumps power, volumetric flow rate, head, and physical size are factors of 5.7, 3.3, 5, and 1.4 lower, respectively, than the 4 EPR primary pumps. However, the AHTR-MI primary pump specific speed is almost identical to EPR, so very similar impellor designs can be used.

3) The AHTR-MI nuclear island has no sources of stored energy that can generate rapid pressure rise, so the AHTR-MI operates with a low-pressure filtered confinement and a below-grade reactor tank silo. This contrasts to the double-shell EPR dry containment building that is designed to sustain an internal pressure of 5.5 bar. The integration of the AHTR-MI IHX's into the reactor tank, rather than use of external steam generators, and the elimination of active safety equipment, reduce the nuclear island volume by a factor of over 2 compared to the EPR.

Table 1-2 Preconceptual design parameter values for AHTR-MI, with comparison to the European Pressurized Reactor (EPR) where applicable.

Parameter	AHTR-MI	EPR
Reactor net electrical power	1100 MW(e)	1650 MW(e)
Reactor thermal power	2400 MW(t)	4500 MW(t)
Power conversion efficiency	~46%	36-37%
Primary coolant	flibe (?)	water
Core inlet temperature	~600°C	296°C
Core outlet temperature	~700°C (?)	327°C
Core power density	10.2 MW(t)/m^3	96.2 MW(t)/m^3
Primary coolant volumetric flow	7.5 m^3/hr MW(t)	25 m^3/hr MW(t)
Primary pump inlet pressure	0.5 bar	155 bar
Primary pump ΔP	~20 m	100 m
Primary pumps power	1.46 kW/MW(t)	8.0 kW/MW(t)
Number of primary pumps	4	4
Primary pumps rotational speed	1200 rpm	1485 rpm
Primary pumps specific speed	4486 rpm$(l/s)^{1/2}m^{-3/4}$	4160 rpm$(l/s)^{1/2}m^{-3/4}$
Primary coolant density	2030 kg/m^3	690 kg/m^3
Primary coolant Prandtl number	16.0	1.0
Primary loop hot leg total flow area	0.000879 m^2/MW(t)	0.0017 m^2/MW(t)
Primary hot leg flow velocity	2.4 m/s	4.1 m/s
Primary hot-leg diameter	0.82 m	1.14 m
Intermediate loop coolant	flinak (?)	water/steam
Intermediate loop/steam generator (SG) inlet temperature	570°C	230°C
Intermediate loop/SG outlet temperature	670°C	293°C
Intermediate heat exchanger/SG power density	50 MW(t)/m^3	4.0 MW(t)/m^3
Intermediate heat exchanger/SG surface area	__ MW(t)/m^2	0.141 MW(t)/m^2
Containment design pressure (EPR—hydrogen deflagration pressure spike)	~ 0 bar	5.5 bar
Nuclear island building volume (a)	32 m^3/MW(t)	75 m^3/MW(t)

a) The nuclear island for AHTR-MI includes: reactor building (34%), fuel building (12%), diesel building (5%), and auxiliary building (49%). This reactor auxiliary building volume is scaled from a PWR counterpart and includes: salt process and storage, control room, and reactor service. Because PWR and AHTR are totally different systems, the AHTR may not an auxiliary building volume this large.

4) The power density of the AHTR-MI reactor core is a factor of 9.4 lower than the EPR, and the AHTR-MI fuel damage threshold temperature is 1600°C. This

results in greater intrinsic safety, but also in increased fuel fabrication costs and spent fuel volume, increasing the relative cost of AHTR-MI fuel recycle and disposal. However, the 25% higher power cycle efficiency of the AHTR-MI improves the sustainability of fuel utilization.

1.3 Upgrade Pathways for the AHTR-MI

The first-generation AHTR-MI is designed to provide a substantial economic advantage over Generation III+ LWRs for electricity production, using similar thermal-spectrum fuel cycles. The first-generation commercial AHTR-MI design will also provide technology to support four primary evolutionary directions:

1) *Power up rates.* The first-generation AHTR-MI design, with modular decay heat removal using PRACS/DRACS, permits future power up-rates to thermal power levels of 4000 MW(t) (1840 MW(e)) without the need to repeat integral effects testing, allowing further capital cost reduction for electricity production.

2) *Hydrogen production.* Design improvements in IHX and primary-loop insulation designs allow future increases in both the core outlet and inlet temperatures, enabling the production of hydrogen by thermochemical and high-temperature electrolysis.

3) *Desalination.* Compared to the low cooling water temperatures required for the EPR's condensing Rankine steam cycle, the high average temperature of heat rejection of the multiple-reheat gas Brayton cycle enables either dry cooling to save water resources, or the generation of additional revenues for desalination using multi-effect distillation.

4) *Actinide management.* The design goal of the first-generation, low-temperature AHTR-MI is to minimize the primary salt inventory, to achieve high efficiency using closed Brayton cycle power conversion, and to use high power-density, low-salt-volume intermediate heat exchangers. This would also provide key technology and operational experience that could be adapted for subsequent design of the Liquid Salt Fast Reactor (LSFR), that could use conventional metallic cladding for fast-spectrum fuels, and for the molten salt reactor (MSR). Such LSFRs and/or MSRs, derived from the low-temperature 2400 MW(t) AHTR-MI, could generate additional revenues by providing actinide management services, and by achieving greatly reduced fuel fabrication and refueling costs compared to conventional thermal and fast reactors.

1.4 References

1.1 C.W. Forsberg, P. Pickard, and P.F. Peterson, "Molten-Salt-Cooled Advanced High-Temperature Reactor for Production of Hydrogen and Electricity," *Nuclear Technology* Vol. 144, pp. 289-302 (2003).

1.2 D.T. Ingersoll, et al., "Status of Preconceptual Design of the Advanced High-Temperature Reactor (AHTR)," Oak Ridge National Laboratory, ORNL/TM-2004/104, May 2004.

1.3 C.W. Forsberg, et al., Proposed and Existing Passive and Inherent Safety-Related Structures, Systems, and Components (Building Blocks) for Advanced Light-Water Reactors, ORNL-6554, October, 1989, pgs. 6-50 – 6-54.

2.0 AHTR-MI PRIMARY SYSTEM DESCRIPTION

This chapter provides an overview of the primary loop design parameters.

Figures 2-1 and 2-2 show preliminary elevation and plan views of the AHTR-MI reactor configuration. Figure 2-3 presents a flow diagram for the AHTR-MI primary loop and reactor tank.

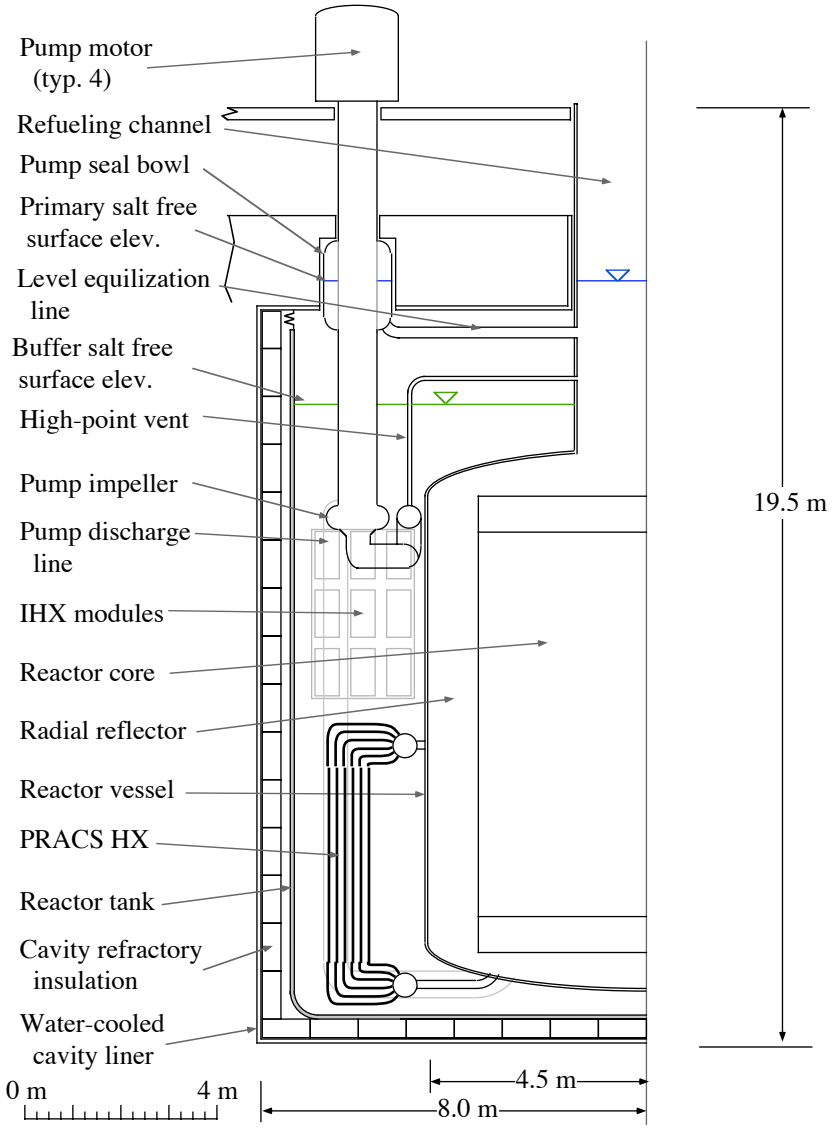

Fig. 2-1 Preliminary AHTR-MI scaled reactor elevation drawing showing locations of primary pumps and IHX modules. (Reactor vessel cover and control-rod drive assemblies that go into the refueling channel are not yet shown).

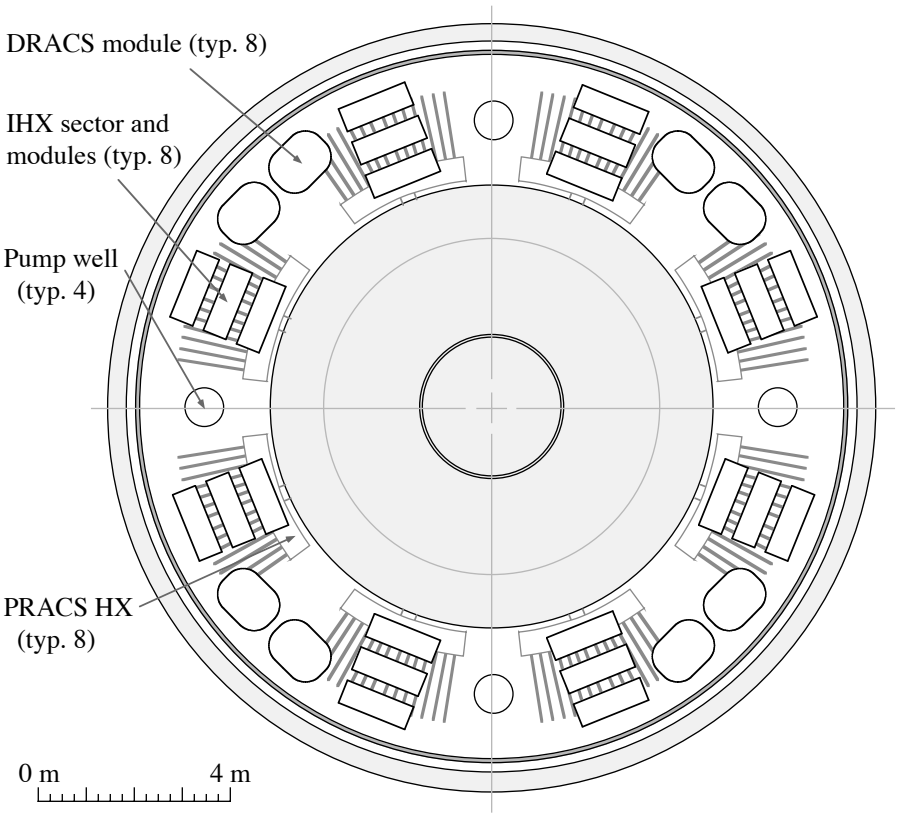

Fig. 2-2 Preliminary AHTR-MI scaled reactor plan drawing showing locations of primary pumps, IHX modules, and DRACS modules.

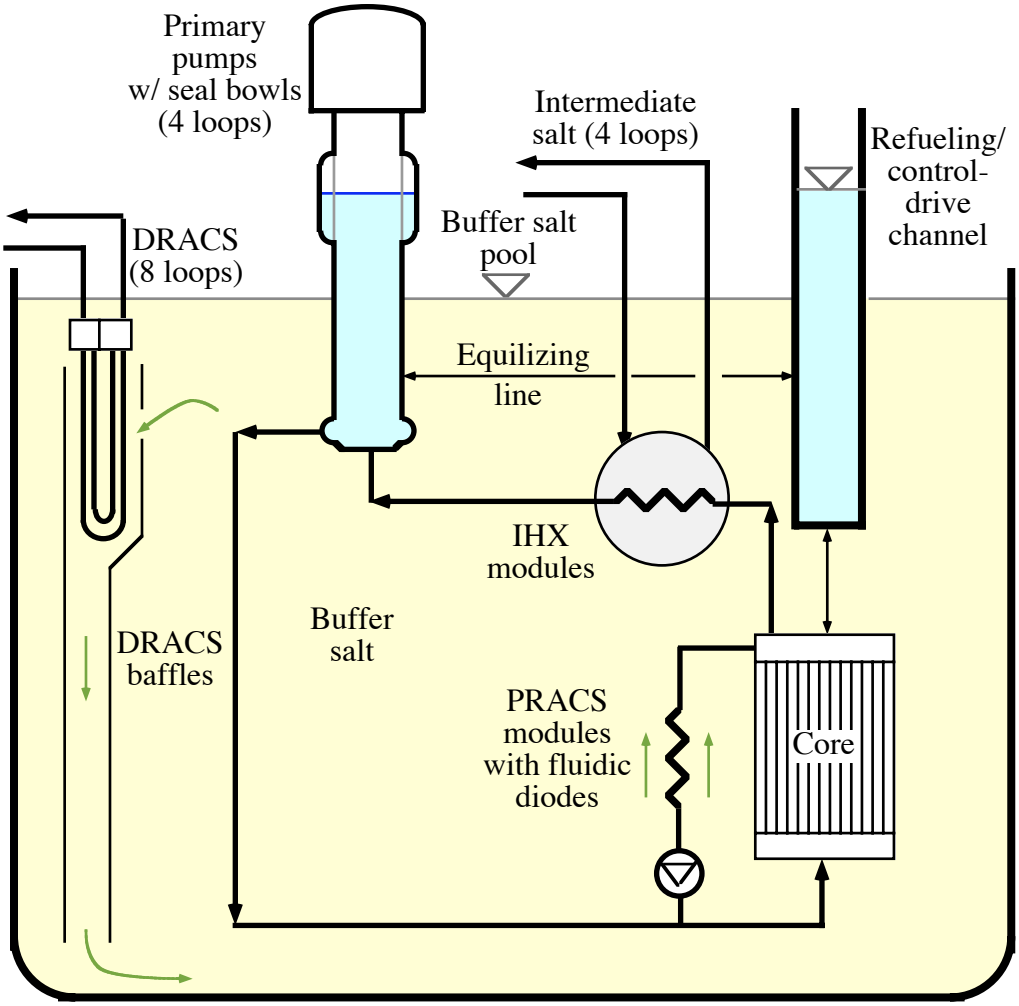

Fig. 2-3 AHTR-MI flow diagram.

3.0 AHTR-MI REACTOR CORE, REFLECTOR, PRIMARY VESSEL AND BUFFER-SALT TANK

This chapter provides a description of the reactor core, reflector, primary vessel and tank design, and the refueling approach for the AHTR-MI. The AHTR-MI design uses the 2005 LS-VHTR core configuration, shown in Fig. 3-1, with baseline parameters summarized in Table 3-1. However, rather than having external intermediate heat exchangers, the AHTR-MI design uses a closed primary loop with compact intermediate heat exchangers immersed in a buffer-salt tank. The closed primary loop is designed to minimize the inventory of primary salt, and therefore the primary vessel and graphite reflector configuration has been based on that developed for the MSBR, which had similar requirements. Section 3.1 reviews the major characteristics of the MSBR primary vessel design. Section 3.2 reviews design issues for the buffer-salt tank.

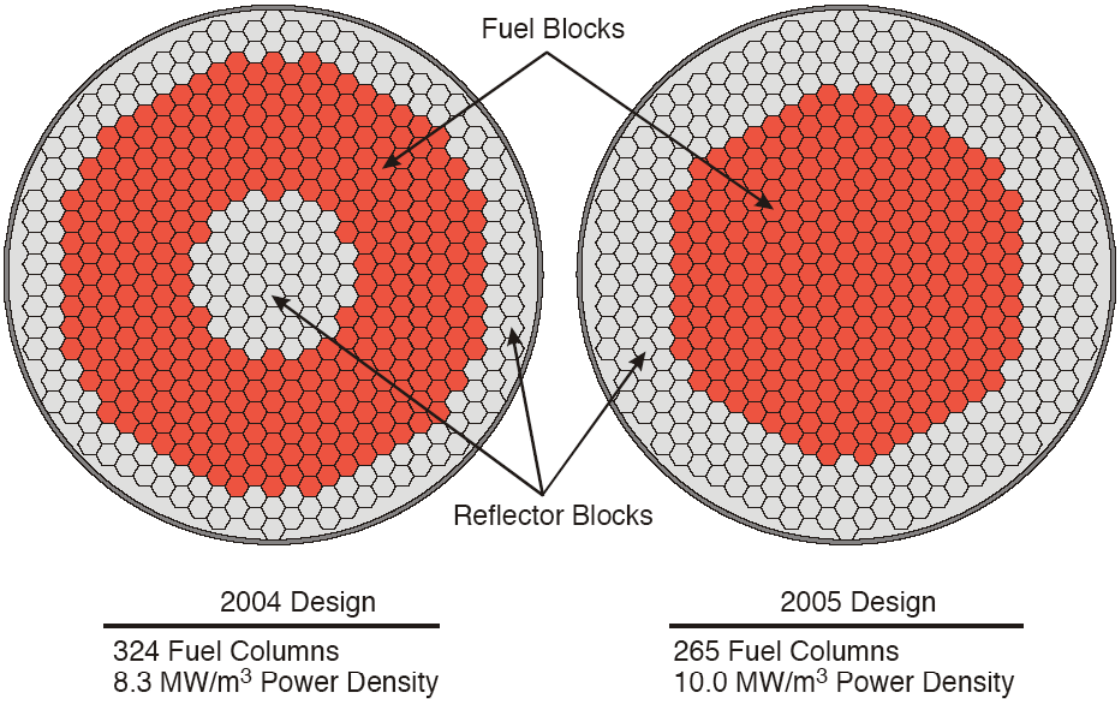

Fig. 3-1 The AHTR-MI design uses the 2005 LS-VHTR reference core configuration [3.1].

Table 3-1 Baseline parameters for the reference AHTR-MI core design [3.1].

Parameter	Value
Coolant salt	$2LiF\text{-}BeF_2$
Li-7 isotopic concentration	99.995%
Outlet coolant temperature	1000°C
Inlet coolant temperature	≥ 850°C
Reactor vessel diameter	9.2 m
Fuel kernel composition	$U_{1.0}C_{0.5}O_{1.5}$
Fuel kernel diameter	425 μm
Particle diameter	845 μm
U-235 enrichment	≤ 20%
Particle packing fraction	≤ 30%
Fuel cycle length	≥ 18 months
Discharge burnup	≥ 100 GWd/t
Fuel element:	
Graphite density	1.74 g/cm^3
Diameter (across flats)	36.0 cm
Height	79.3 cm
Fuel channel diameter	1.27 cm
Number of fuel channels	216
Coolant channel diameter	0.953 cm
Number of coolant channels	108
Pitch between channels	1.88 cm
Power density	10.0 MW/m^3
Number of fuel columns	265
Number of fuel blocks per column	10

3.1 AHTR-MI Primary Vessel Design

The MSBR reactor vessel and graphite reflector system were designed to minimize the total inventory of fuel salt flowing through the graphite moderator blocks ([3.2], pg. 10). The AHTR-MI primary loop has similar design requirements, although the square moderator blocks of the MSBR are replaced by hexagonal fuel assemblies.

The 2250 MW(t) MSBR reactor vessel, shown in Figs. 3-2 and 3-3, was 6.7 m (22 ft) in diameter and 6.1 m (20 ft) high, and was designed for an internal pressure of 5.1 atm (75 psig). It had 5-cm thick walls, and 7.5-cm thick dished heads at the top and bottom. Fuel salt entered at 566°C (1050°F) through four 0.40-m (16 in) diameter nozzles through a lower plenum and upward through passages in graphite moderator blocks, to exit at the top at 704°C (1300°F) through four equally spaced nozzles which connected to 0.51 m (20 in) suction nozzles leading to circulation pumps.

The 2400 MW(t) AHTR-MI vessel is larger than the MSBR, with the current design (Fig. 2-1) having a diameter of 9.0 m and a height of 11 m, versus 6.7m and 6.1 m respectively for the MSBR.

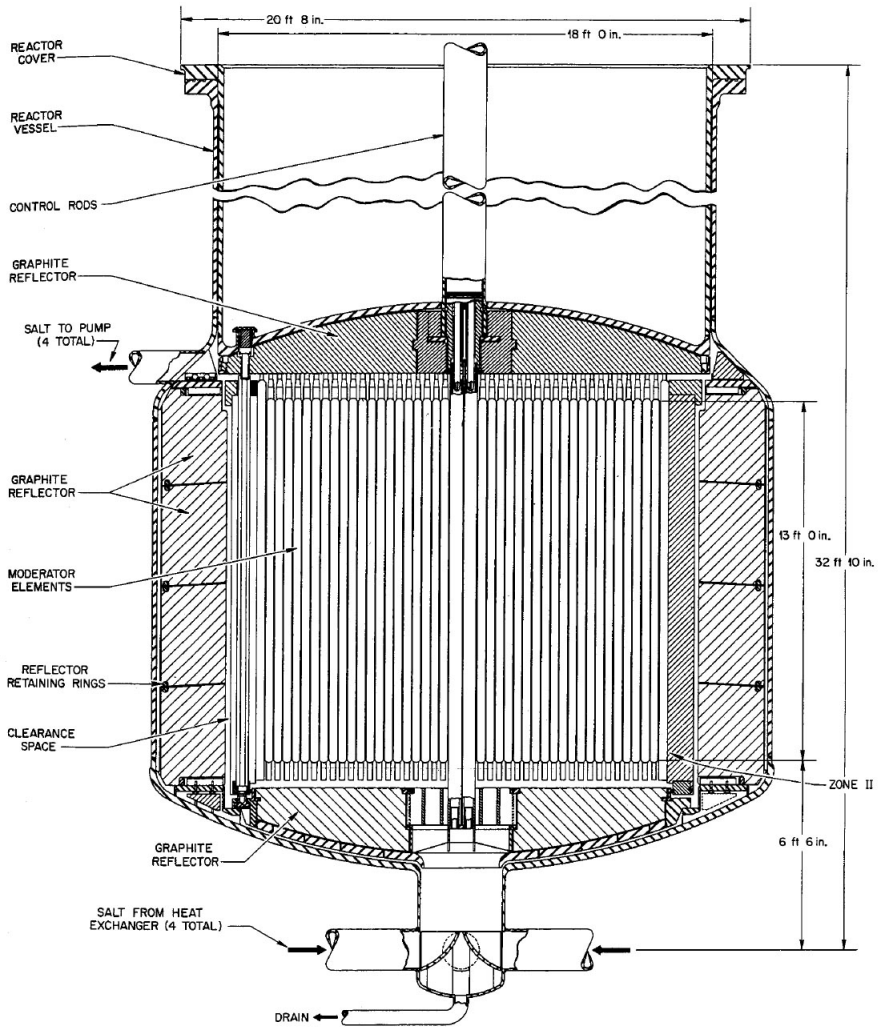

Fig. 3-2 Elevation view of the MSBR reactor vessel, and reflector and moderator elements [3.2].

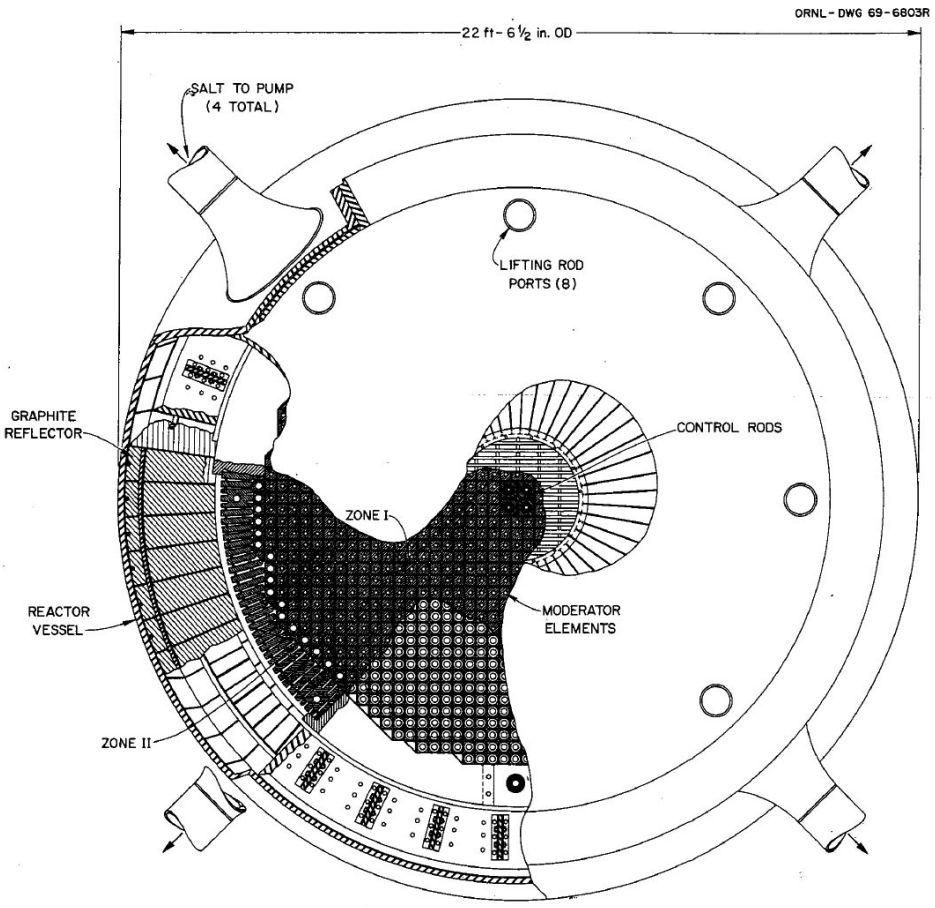

Fig. 3-3 Elevation view of the MSBR reactor vessel, and reflector and moderator elements [4.2].

3.2 AHTR-MI Reactor Tank Design

The initial design of the AHTR used the S-PRISM reactor vessel design. The S-PRISM uses a seismically isolated, 9-m diameter, 20-m high pool-type reactor vessel and guard vessel that are suspended. However, for the AHTR there is a need to go to higher normal and peak vessel temperatures, and the buffer salt is about 3 to 4 times more dense than sodium, leading to the need for much thicker vessel walls and difficulty with fabrication using the S-PRISM approach.

The main differences between AHTR and S-PRISM are the coolant. The AHTR has (1) a transparent liquid salt, which should allow visual in-service inspection of the inside of the AHTR vessel and its internal structures using actively cooled video cameras, and (2) in contrast with sodium liquid salts are quite benign with water, allowing the AHTR to use water cooling for the walls of the reactor cavity. This may allow a different and simpler vessel, or tank, to be used.

The current reference design of the AHTR-MI uses an underground, cylindrical concrete silo to hold a flat-bottomed reactor tank. The silo is steel lined, and has an

active water cooling system using embedded tubes below the liner, using the same design approach for cooling the liner as has been used in reinforced concrete HTGR vessels like Fort St. Vrain. The liner incorporates an internal drip collection system as is used in the HTRGs to detect any condensation or collection of moisture. During severe accidents where the tank would rupture, boiling of water in the cavity cooling system would continue to remove heat from the liner, and thus provide the ultimate heat removal method. If the cavity cooling system fails, heat removal continues by conduction into the thermal mass provided by concrete silo.

During normal operation, the cavity cooling system removes a modest fraction of heat from the reactor tank. The silo is lined with refractory insulating blocks on its bottom and side (possibly low-thermal conductivity graphite) to reduce this heat removal rate, and thus the tank is largely isothermal, reducing thermal stresses. The primary mechanism for decay heat removal from the buffer salt is then modular DRACS loops. Heat rejection by these loops and the cavity cooling system can maintains the buffer salt at a temperature below the temperature of the primary loop, so that the normal operating temperature of the reactor vessel can be maintained modestly above the salt freezing temperature (say a normal operating temperature of 550°C) to increase the thermal inertia available from the buffer salt and to reduce thermal creep of the reactor tank and of primary loop components that contact the buffer salt.

The vessel is a flat-bottomed tank. Construction may be from a high-temperature alloy like Alloy 800H with a corrosion-resistant cladding on the inside. At the center of the tank bottom, there is a pin that aligns the tank to be centered in the cavity. The tank rests on the refractory blocks lining bottom of the cavity. While the tank bottom is pinned at the center, to accommodate radial thermal expansion the tank slides on the surface of the blocks. All gravity loads from the tank, primary salt, and reactor internals are then transferred through the tank bottom and insulating blocks to the bottom of the cavity.

The tank walls do not carry vertical gravity load, as in the S-PRISM. Instead, the tank walls would primarily carry hoop stresses associated with the hydrostatic head of the liquid-salt pool. This reduces the stresses in the tank wall by 33% to 50%, compared to the S-PRISM vessel design.

While the reactor cavity will be largely isothermal, there will likely be some vertical temperature gradients in the tank due to thermal stratification in the liquid salt pool. To strengthen the tank against hoop stresses and to provide connection locations for snubbers that may be required to transfer horizontal seismic loads, the tank design may incorporate external circumferential stiffening rings. These help to increase the tank strength to hoop stresses, while minimizing thermal stress generation due to vertical temperature gradients in the tank wall.

The concrete reactor silo will be seismically base isolated, which will reduce horizontal seismic loads. Horizontal loads for reactor internals may be transferred through the center pin at the bottom of the tank, and potentially transferred by snubbers located inside the tank as well, through the tank wall to the vessel cavity snubbers. These snubbers must be capable of operating submerged in liquid salt and accommodate

differential thermal expansion of reactor internal structures and the tank wall, while locking rigidly from rapid motions.

Wave motion induced at the pool surface due to seismic force complicates the dynamic response of the tank. Baffling that would transfer horizontal forces more uniformly through the liquid may be useful to reduce tank sloshing effects and to increase the sloshing resonant frequency.

3.3 AHTR-MI Core Reflector Design

The AHTR-MI core reflector design is derived from the MSBR. Figure 3-4 shows the configuration of the graphite reflector blocks and the cooling channels used in the MSBR to maintain them at a temperature near the core inlet temperature.

The flow pattern through the graphite reflector blocks and reactor core is designed to be very similar to that used in earlier designs of the Molten Salt Reactor (MSR). In these designs, typified by the design of the Molten Salt Breeder Reactor where cool salt flows in the region of the graphite reflector, isolating the metallic reactor vessel from the heated salt flowing through the core, and maintain the metallic vessel at a nearly constant temperature. Extensive design was performed [3.2] addressing issues such as the optimal geometry of graphite reflector blocks, methods to remove and install replaceable graphite reflector and moderator elements, and methods to address the differential thermal expansion of metallic and graphite components and graphite dimensional changes under irradiation. This experience may be applied to design the reflector, core support, and outlet plenum of the AHTR-IT.

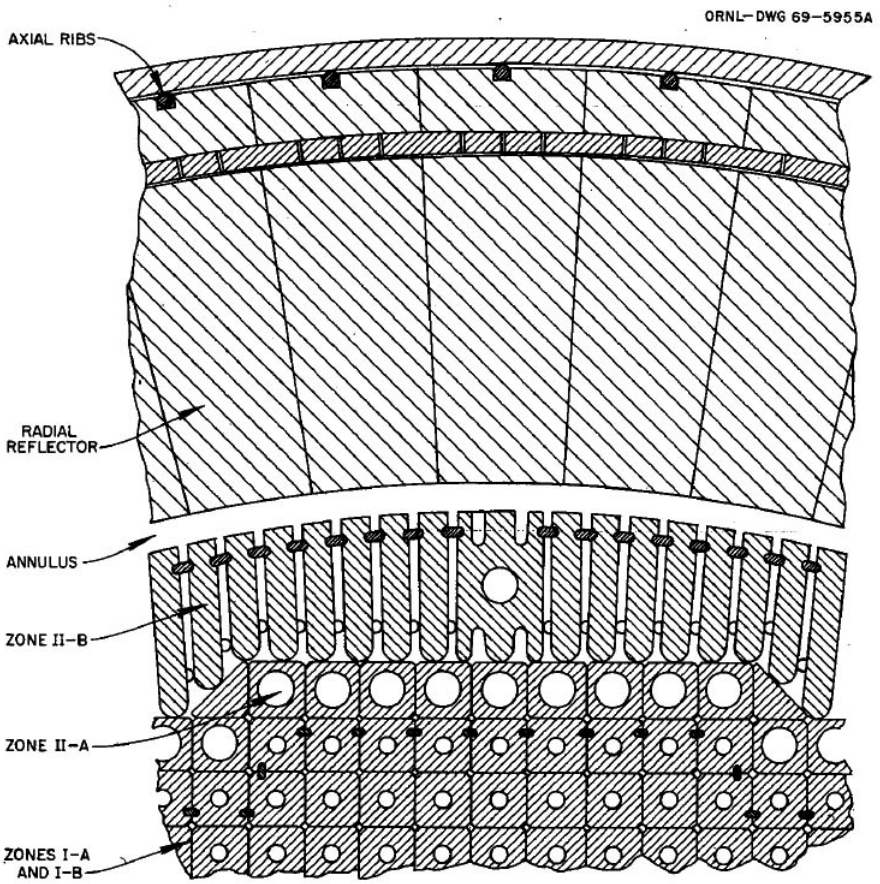

Fig. 3-4 Detail of the MSBR reactor vessel reflector and moderator elements [3.2].

3.4 References

4.1 D. T. Ingersoll, et al., "Status of Physics and Safety Analyses for the Liquid-Salt-Cooled Very High-Temperature Reactor (LS-VHTR)," Oak Ridge National Laboratory, ORNL/TM-2005/218 (Draft) September 2005.

4.2 R.C. Robertson, 6/71 "Conceptual Design Study of a Single-Fluid Molten-Salt Breeder Reactor," Chapter 3, "Reactor Primary System," ORNL-4541, June, 1971.

4.0 AHTR-MI INTERMEDIATE HEAT EXCHANGERS

This chapter reviews the design of the AHTR-MI intermediate heat exchanger (IHX) system. The AHTR-MI uses high power density compact heat exchangers immersed under the surface of the buffer-salt pool. Figures 4-1 and 4-2 show the diffusion-bonded, offset strip fin Heatric type heat exchanger that provides the baseline for the AHTR-MI IHXs.

The current design goal for the AHTR-MI IHX's is to achieve a power density of 50 MW(t)/m^3 with a ~30°C log mean temperature difference (LMTD) between the primary and intermediate salts. This results in a total volume of 48m^3. Currently, it is recommended that there be 8 IHX sections arranged symmetrically around the reactor tank annulus. Cooled primary salt from 2 IHX sections then is ducted to the suction of a single primary pump (Chapter 6). Each IHX section has 10 IHX modules, each rated at 30 MW(t), with banks of 5 modules located at two elevations.

Each of the 8 IHX sections receives hot flow from a hot duct exiting the top of the primary core vessel. The hot ducts and cross-over ducts to the IHX's are arranged to vent and collect gases at a low-velocity high point in the cross-over duct. A vent line is provided to purge gas to the refueling channel, and to equalize the pressure of the pump suction with the refueling channel.

Fig. 4-1 Photo of a cutaway-model of a typical Heatric heat exchanger showing multiple inlet and outlet manifolds and slices across various plates and flow channels.

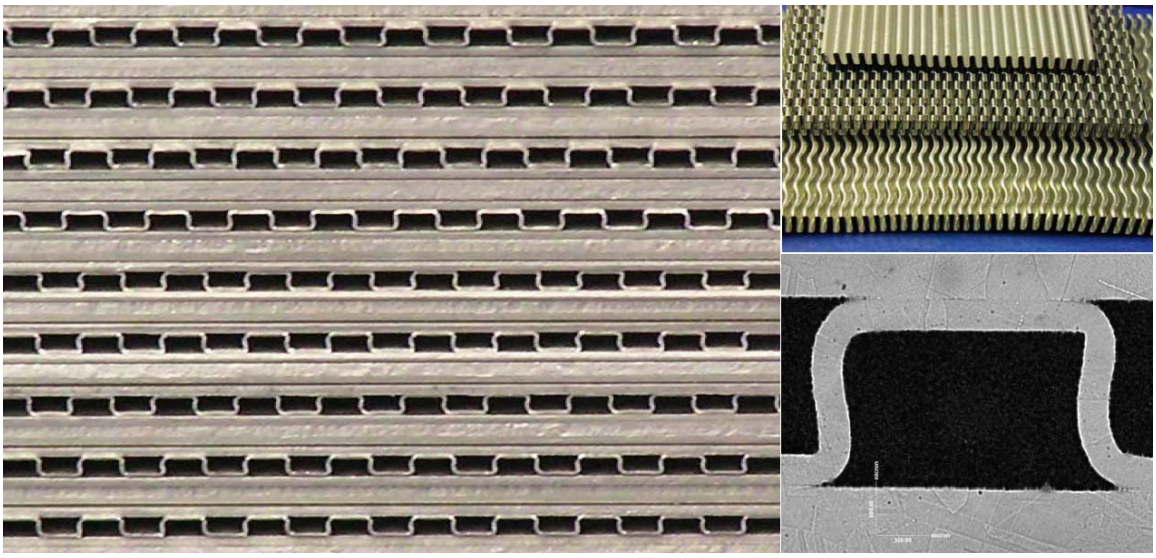

Fig. 4-2 Diffusion bonded formed plate heat exchanger (FPHE).

5.0 AHTR-MI PRIMARY PUMPS

The AHTR-MI primary pumps have similar requirements to the vertical shaft, single-stage centrifugal pump designs that were developed in the early 1970's for the Molten Salt Breeder Reactor (MSBR). As shown in Table 5-l, the AHTR-MI uses very similar primary coolant flow rates as the MSBR, but requires lower pump head, power and shaft torque. The higher specific speed of the AHTR-MI primary pump, compared to the MSBR, is comparable to that typical of PWR primary pumps (for example see the comparison with the EPR in Table 1-2). Figure 5-2 shows a cut-away view of the EPR primary pump. The higher specific speed results in the use of a mixed-flow impellor design as shown in Fig. 5-1, which can be more readily designed using current fluid dynamics modeling tools than was possible at the time of the MSBR project.

Table 5-1 Comparison of general pump requirements for the 8 MW(t) MSRE and 2250 MW(t) MSBR systems ([5.1], pg. 223) with the 2400 MW(t) AHTR-MI.

	MSRE		**MSBR**		**AHTR-MI**	
	Primary	Secondary	Primary	Secondary	Primary	Secondary
Number of salt loops	1	1	3-4	3-4	4	4
Design temperature (°C)	700	700	700	700		
Pump capacity (m^3/hr)	272	193	4,770 – 3,630	5,220 – 4,540	4,460	
Head (m)	15.2	30.5	45.7	91.4	20	
Speed (rpm)	1150	1750	1190	1150	1200	
Specific speed N_S $(rpm(l/s)^{1/2}m^{-3/4})$	1300	955	1840 - 1607	1660 - 1427	4470	
Net positive suction head required (m)	3.0	3.0	6.4 - 5.5	11.3 - 9.1		
Impellor input power (kW)	35.8	33.6	2160 - 1640	3050 - 2310	880	

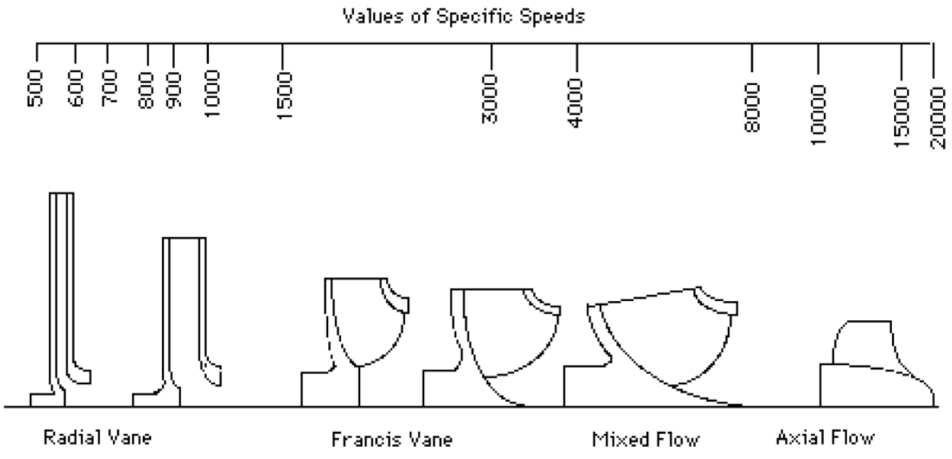

Fig. 5-1 Effect of specific speed $(rpm(l/s)^{1/2}m^{-3/4})$ on impellor geometry.

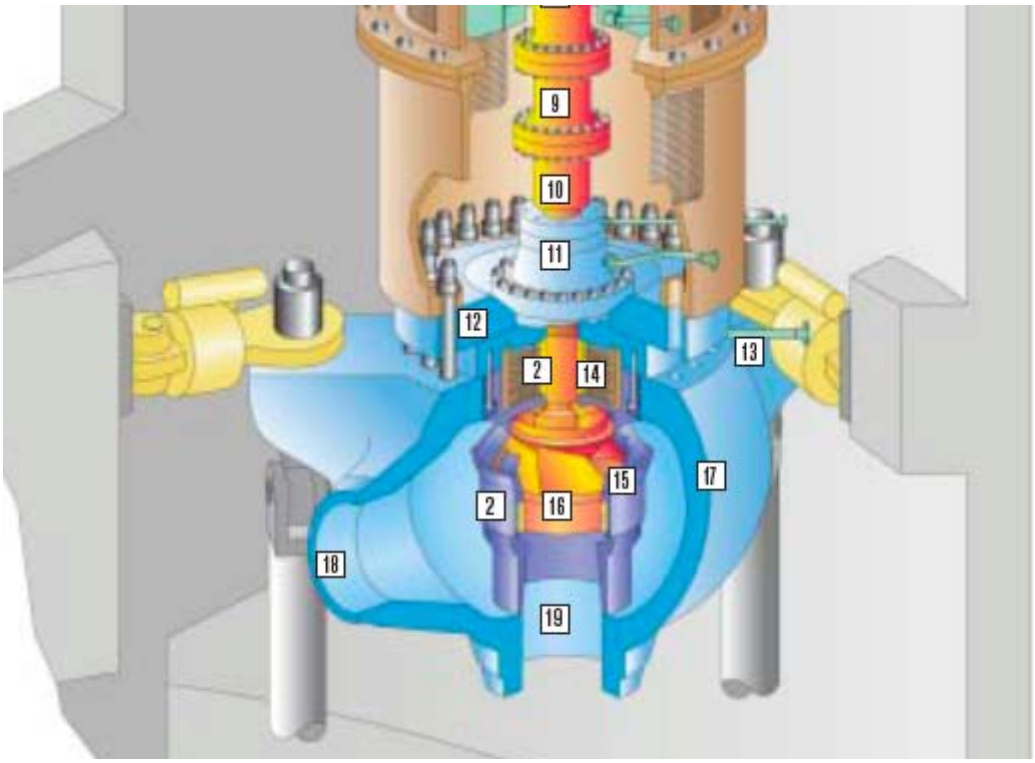

Fig. 5-2 Vendor's brochure figure for the EPR primary pump, showing the suction (19), discharge (18), a mixed flow impellor (16) and two water-lubricated bearings (2). Other components include a spool piece (9), pump shaft (10), shaft seal housing (11), main flange (12), seal water injection (13), thermal barrier heat exchanger (14), and diffuser (15).

Very large programs have been conducted to develop high-temperature centrifugal pumps for liquid metal and molten salt applications. References [5.1] and [5.2] summarize the major results from the MSBR pump development program, and are recommended as the best references for reviewing the technology. More recently, substantial development has occurred for molten salt pumps for nitrate salts, with the development and testing of nitrate-salt-lubricated bearings working up to 565°C [5.3].

For liquid-salt applications, liquid seals like those used on PWR pumps cannot be used. In the MSRE and MSBR programs, the shafts passed through a salt/inert gas free surface, allowing gas seals to be used. The pump impellors were cantilevered, so that conventional oil-lubricated bearings and gas seals could be applied. Figure 5-2 shows the short-shaft pump design that was created and became the baseline design for the MSBR project. The short-shaft design has the advantage of not requiring a salt-lubricated bearing, but as seen in Fig. 5-3, this results in the impellor elevation being less than 0.2 below the salt free surface. Limited work was performed to develop salt-lubricated bearings that would permit the use of long-shaft pumps. Figure 5-4 shows a representative design. Recent work for nitrate salt pumps, like that shown in Figure 5-5, has shown the practicality of long-shaft designs [5.3], but additional work will be required to develop and qualify bearing materials for use with fluoride salts.

Because the AHTR-MI requires the use of multiple primary pumps, it faces the problem maintaining equal liquid levels for the free surfaces in the four primary pump seal bowls and in the refueling channel. Furthermore, the MSBR was capable of draining its fluid fuel to provide long-term decay heat removal, allowing the primary pumps to be located less than 0.5 m below the liquid free surface. Conversely, for the AHTR-MI a natural circulation flow path must be maintained even if a the primary loop ruptures and the levels of the primary and buffer salts equilibrate, and even if the reactor tank ruptures and the levels of both the primary and buffer salts drop. To keep the primary pump impellor submerged even with a primary-loop rupture, the primary pump impellor likely must be located 1 to 3 m below the liquid free surface, as shown in Figure 2-1. This in turn likely necessitates the use of salt lubricated bearing, and the necessity to have the high-temperature length of the pump shaft be longer and thus subject to larger thermal distortions.

In developing the design of the AHTR-MI primary pumps, based upon the MSBR designs as a starting point, it will be important to review areas where technologies have changed and improved since the MSBR pump designs were studied. These include new capabilities for variable speed motors, for flexible couplings, and for impellor and bearing designs.

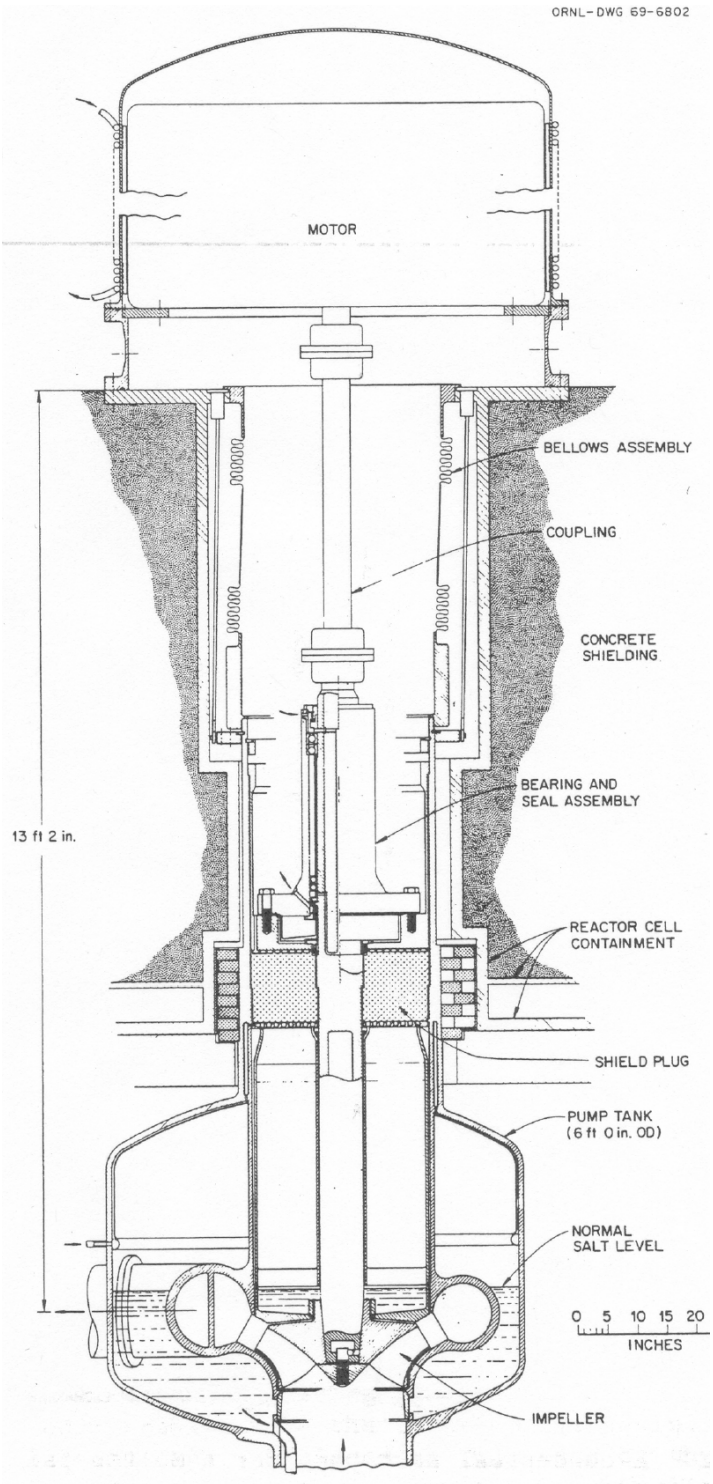

Fig. 5-3 MSBR "short-shaft" primary pump design ([5.1], pg. 227)

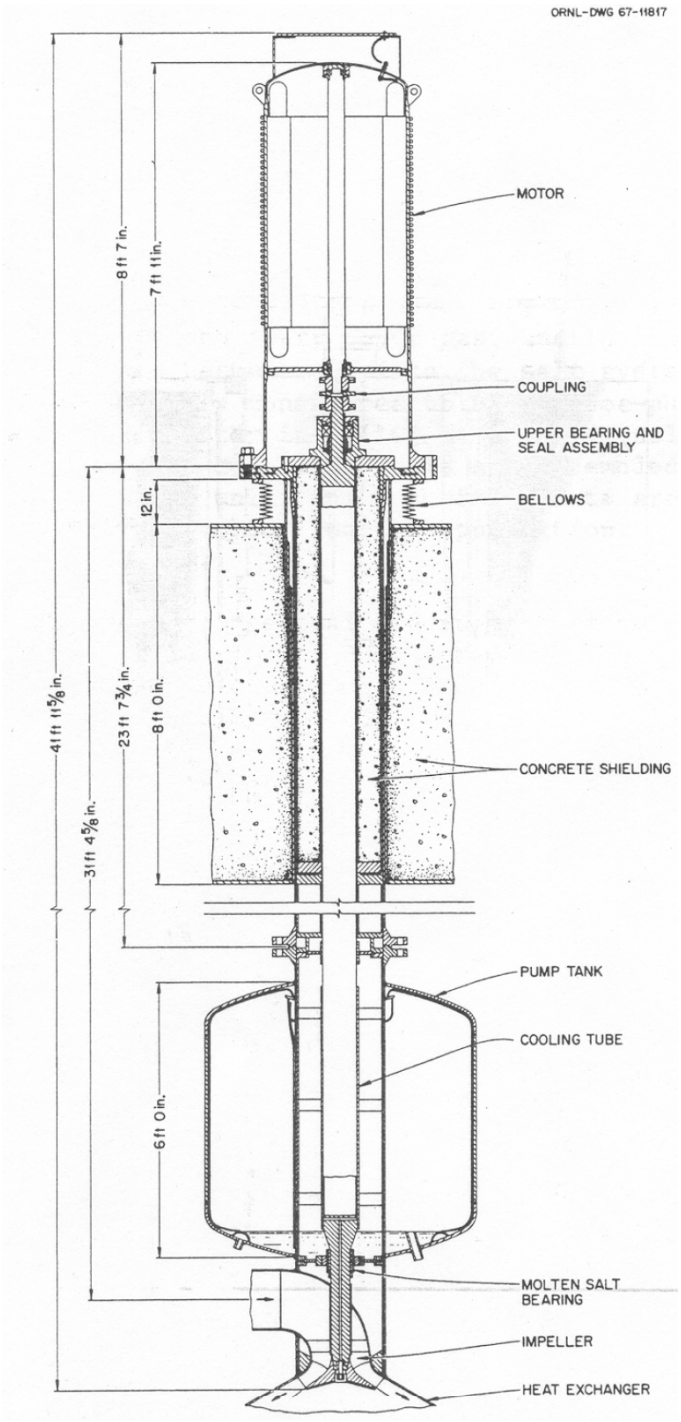

Fig. 5-4 MSBR "long-shaft" primary pump design ([5.1], pg. 228)

Fig. 5-5 Nagle long-shaft nitrate molten salt pump used to test salt-lubricated bearings for 5000 hours at 565°C [5.3].

5.1 References

5.1 ORNL 4812, pp. 222, August 1972. (see PDF file: MSR.ORNL-4812_PumpValve.pdf)

5.2 EBASCO pump report, Dec. 1971, (see PDF file: MSR.Ebasco_PumpValve.pdf).

5.3 D.L. Barth , J. E. Pacheco, W. J. Kolb, and E. E. Rush, Development of a High-Temperature, Long-Shafted, Molten-Salt Pump for Power Tower Applications, Journal of Solar Energy Engineering, Vol. 124, pp. 170-175, May 2002.

6.0 AHTR-MI SAFETY AND PIRT ANALYSIS

The system transient response must be understood for normal operation modes, anticipated transients, and accidents. This chapter outlines the potential transients and accidents that may be considered when the preliminary Phenomena Identification and Ranking Tables are developed for the LS-VHTR and AHTR-MI. These will include:

Normal operation modes
- Steady-state power operation
- Startup/shutdown transients
- Hot standby with primary pumps stopped
- Cold standby
- Refueling

Anticipated transients
- Loss of forced cooling (no intermediate cooling or primary pump operation)
- Loss of flow in 1 or more primary pumps
- Loss of intermediate loop flow to one or more IHX modules
- Abrupt change of intermediate loop inlet temperature to one or more IHX modules
- Pinhole flow leakage in an IHX resulting in addition of intermediate salt to the primary loop
- Loss of cover-gas inerting

Accidents
- Primary pipe break inside reactor vessel
- Intermediate loop pipe break, draining into vessel
- DRAC module pipe break draining into vessel
- Reactor vessel breach and leakage
- Others (comprehensive survey needed)

7.0 AHTR-MI PILOT PLANT

A scaled 35 to 75 MW(t) AHTR pilot plant is planned. This chapter presents a preliminary core configuration for the AHTR-MI pilot plant. The key role of the pilot plant is to reproduce the major phenomena that must be understood in order to reliably design, license, and construct a full-scale demonstration plant. Because the pilot plant will be reduced power and reduced height compared to the full-scale plant, its natural circulation thermal hydraulics will be better reproduced by adopting accelerated time scaling, and therefore higher core power density (15.0 MW/m^3) than that of the full-scale plant (10.2 MW/m^3). This higher power density will also allow radiation-damage related phenomena to be accelerated in the pilot plant.

The pilot plant uses prismatic fuel blocks of the same size and design as the prototypical fuel. Each fuel block is 0.36 m across, from flat to flat, and 0.79 m high, with a volume of 0.089 m^3. Figure 7-1 shows the baseline pilot-plant core design, which is 5 fuel blocks wide and has a total of 19 fuel blocks in each row. The two design variations for the pilot plant consist of a low-aspect ratio core consisting of two rows of blocks (38 total) and a high aspect ratio design with three rows (57 blocks total). The power density will range from the prototypical power density of 10.2 MW/m^3 up to a high power density of 15 MW/m^3. The potential power level of the pilot plant then ranges from 35 MW(t) (2-row, 10.2 MW/m^3) to 75 MW(t) (3-row, 15 MW/m^3).

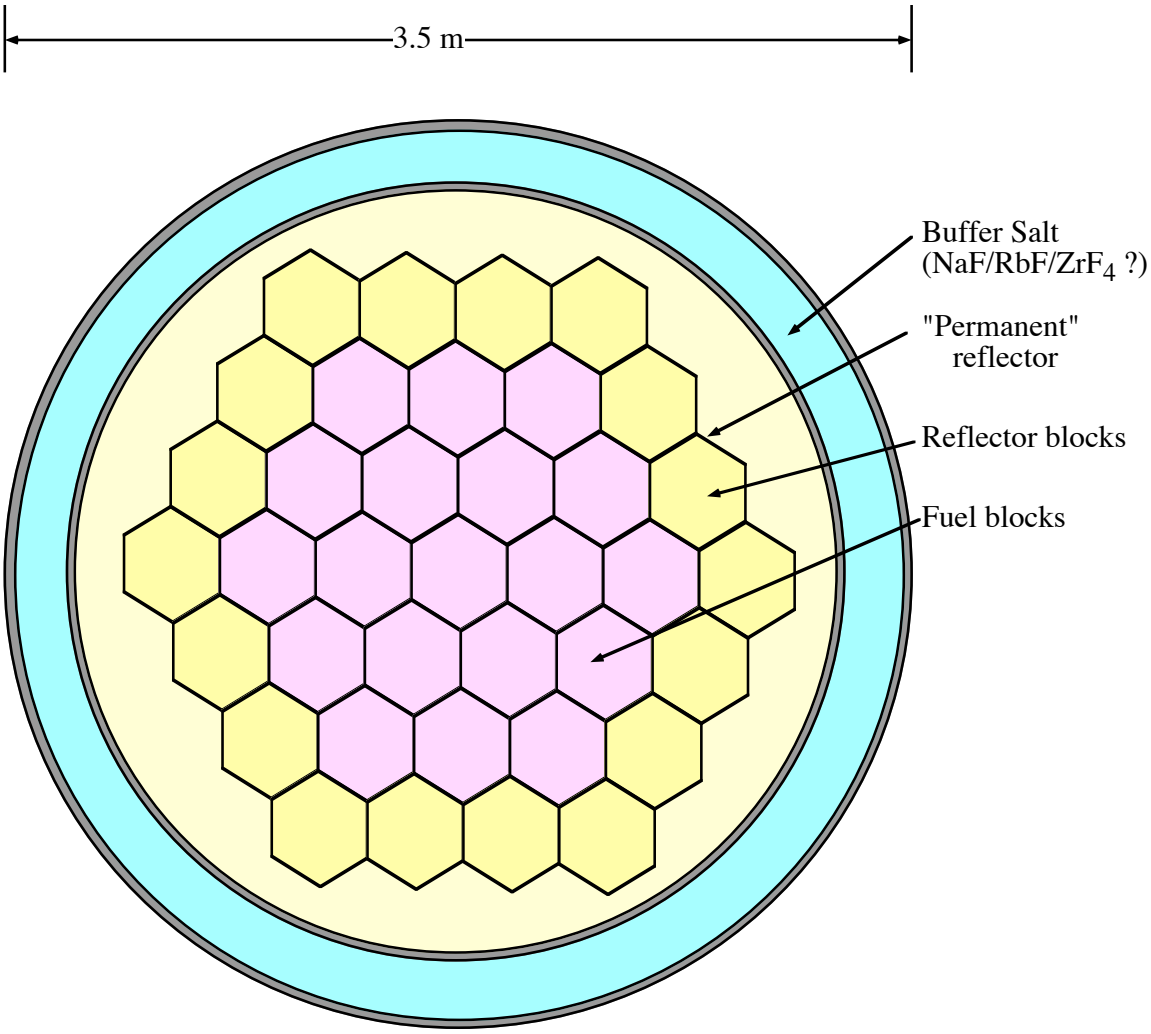

Fig. 7-1 Cross section of the baseline AHTR-MI pilot plant core